

SEQUENTIAL MONTE CARLO RADIO-FREQUENCY TOMOGRAPHIC TRACKING

Yunpeng Li[†], Xi Chen^{*1}, Mark Coates^{*} and Bo Yang[†]

[†] Multimedia Technology Center, Beijing Univ. of Posts and Telecom., Beijing, China

^{*} Dept. of Electrical and Computer Engineering, McGill University, Montreal, Quebec, Canada
E-mail: liyp@bupt.edu.cn; xi.chen8@mail.mcgill.ca; mark.coates@mcgill.ca; boyang@bupt.edu.cn

ABSTRACT

Radio Frequency (RF) tomographic tracking is the process of tracking moving targets by analyzing changes of attenuation in wireless transmissions. This paper presents a novel sequential Monte Carlo (SMC) method for RF tomographic tracking of a single target using a wireless sensor network. The algorithm incorporates on-line Expectation Maximization (EM) to estimate model parameters. Based on experimental measurements, we introduce a new measurement model for the attenuation caused by a target. We assess performance through numerical simulation and demonstrate that it significantly outperforms previous RF tomographic tracking procedures.

Index Terms— RF Tomography, On-line EM, Sequential Monte Carlo, Wireless Sensor Networks

1. INTRODUCTION

Device-free passive (DfP) localization techniques estimate the locations of moving objects without requiring that the objects carry devices that transmit or reflect signals [1]. Many different DfP algorithms have been developed in recent years. Signature-based algorithms can be effective but require extensive training data to learn signal patterns that correspond to target positions. Radio-frequency tomographic imaging/tracking avoids this by proposing a statistical model for the change induced in the mean (or variance) of the received signal strength of a transmission when a target is present between the wireless transmitter and receiver [2, 3, 4, 5].

RF tomographic imaging involves an image reconstruction step to estimate target locations [2, 3]. The only previous RF tomographic tracking approach [3] treats the maximum of this image as a “measurement” and applies a Kalman filter to track the target. This method has several disadvantages: (i) it necessitates a pixelization of the region of interest (to form an image); (ii) an imaging problem must be solved, which is considerably more challenging than the actual tracking problem of interest; (iii) the measurements are artificial and the pixelization induces an undesirable quantization error.

We propose a novel RF tomographic tracking algorithm, which avoids the imaging task. We adopt a particle filtering (Sequential Monte Carlo) approach. In order to make the algorithm computationally efficient and improve tracking accuracy, we introduce a new measurement model, whose form is motivated by experimental data. This model does not pixelize the region of interest, in contrast to the measurement models of [2, 3]. Our algorithm incorporates an on-line Expectation Maximization (EM) procedure to estimate the parameters of the dynamic model of the target and the observation

model. These parameters can vary significantly for different targets and environments, so the on-line EM algorithm provides an important self-calibration mechanism.

The rest of the paper is organized as follows. Section 2 provides a problem statement. Section 3 describes the pixel-free measurement model and Section 4 details the new algorithm. Section 5 reports on simulation experiments and Section 6 makes concluding remarks.

2. PROBLEM STATEMENT

When RF signals are transmitted through a sensed area, the obstructions inside the area can absorb, scatter or reflect part of the signals. These effects cause attenuation of the Received Signal Strength (RSS). The changes in mean attenuation of the signals transmitted between multiple pairs of sensor nodes can be used to estimate the position of a moving target.

We consider a network of N nodes and M links. In each measurement interval, the N nodes successively broadcast packets and the neighboring nodes measure the RSS. The RSS value of link i at time step k is $y_i(k)$. We assume that we have access to a relatively small number of sensor measurements recorded during a period when there is no object moving through the sensed area. From these, we calculate an average background RSS value vector \mathbf{y}_{avg} , which contains the average RSS values across all links:

$$\mathbf{y}_{\text{avg}} = [\bar{y}_1, \bar{y}_2, \dots, \bar{y}_M]^T \quad (1)$$

This vector captures the attenuation caused by the stationary objects in the region of surveillance.

During the tracking period, an instantaneous RSS value vector \mathbf{y}_k is collected from the sensors at time k . This contains an RSS value for each of the M links. We subtract the background vector \mathbf{y}_{avg} to obtain a vector of the RSS change:

$$\mathbf{z}_k = \mathbf{y}_k - \mathbf{y}_{\text{avg}} \quad (2)$$

Our goal is to track a single moving target described by state \mathbf{x}_k , with motion specified by a Markovian dynamic model $f(\mathbf{x}_k|\mathbf{x}_{k-1})$. In order to do this, we strive to maintain a particle approximation of the marginal posterior $p(\mathbf{x}_k|\mathbf{z}_{1:k})$ and estimate the expected value of \mathbf{x}_k under this distribution.

3. MEASUREMENT MODEL

The measurement model describes the relationship between the true state and the measurement values. In this paper, we propose a pixel-free measurement model for the attenuation caused by a target moving between a transmitter s and receiver r . The model is motivated by experimental data recorded in a sensor network deployed in an

¹Xi Chen and Yunpeng Li are considered as equal first authors

This research is supported by Special Foundation of International Science and Technology Cooperation and Exchange of China (2008DFA12300).

outside environment with relatively few obstructions (some trees and a statue). Figure 1 shows the data we recorded together with the model we propose, where the two parameters of the model have been chosen by simple regression to minimize the mean-squared error.

For the two-way link i between a node pair, consider an ellipse with foci at the transmitter and receiver. Define:

$$\lambda_k^i \triangleq d_i^s(\mathbf{x}_k) + d_i^r(\mathbf{x}_k) - d_i \quad (3)$$

where $d_i^s(\mathbf{x}_k)$, $d_i^r(\mathbf{x}_k)$ are the distances from the target's position to the source and receiver, respectively, and d_i is the link distance. λ_k^i is a parameter related to link i 's elliptic width which describes the target's position relative to the link i at time step k .

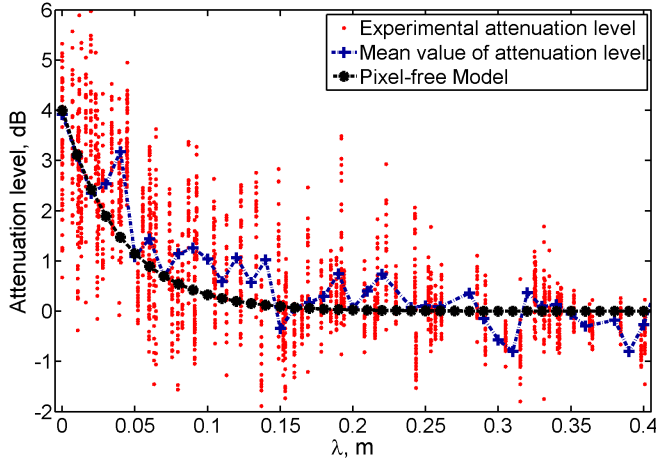


Fig. 1. Attenuation level versus λ for the proposed pixel-free model: a comparison between the model and experimental measurements.

We define an $M \times 1$ vector $\mathbf{g}_k \triangleq [g_k^1 \dots g_k^i \dots g_k^M]^T$ where

$$g_k^i \triangleq \begin{cases} e^{-\frac{\lambda_k^i}{2\sigma_\lambda}}, & \lambda_k^i \geq 0 \\ 0, & \text{otherwise.} \end{cases} \quad (4)$$

Here σ_λ is a parameter that controls the rate of decay of attenuation with respect to λ . We then construct the pixel-free measurement model as

$$\mathbf{z}_k = \phi \mathbf{g}_k + \sigma_s \mathbf{S}_k \quad (5)$$

where \mathbf{z}_k is a $M \times 1$ vector represents the measured attenuation, ϕ is a scalar weight parameter, and \mathbf{S}_k is a $M \times 1$ vector of measurement noise with $\mathbf{S}_k \sim N(0, I_{M \times M})$.

4. SMC RF TOMOGRAPHIC TRACKING ALGORITHM

We employ a particle filter to track the marginal posterior distribution $p(x_k | z_{1:k})$. The filter maintains a weighted particle approximation to the marginal posterior (see [6] for a tutorial introduction and overview of particle filtering techniques). In this paper, we describe a sequential importance resampling (SIR) approach, but it is also possible to use other methods such as auxiliary particle filtering.

The observation model that we outlined in Section 3 has three unknown parameters, ϕ , σ_λ , and σ_s . Our experimental experience with the second of these parameters σ_λ is that it is relatively consistent for different targets and environments. We therefore choose to

estimate it from our experimental data and fix it as a constant in our tracking algorithms. There is considerably more variation in ϕ and σ_s . For this reason, we choose to estimate these using the on-line Expectation-Maximization (EM) approach described in [7].

We adopt a Gaussian AR-1 model for the target dynamics, i.e. $\mathbf{x}_{k+1} = a\mathbf{x}_k + \sigma_v \mathbf{v}_k$, where \mathbf{x}_k is the target position in the 2D plane and $\mathbf{v}_k \sim N(0, 1)$. The constant $a < 1$ models a (small) drift towards the centre of the surveillance region and leads to a stationary process; we choose a as a constant that is close to 1.

4.1. On-line EM Algorithm

In the on-line EM algorithm, we form estimates of the set of parameters $\theta = [\phi, \sigma_s, \sigma_v]$. Here we provide a necessarily brief overview of the on-line EM algorithm. We refer the reader to Section III.B of [7] for more detail.

A natural approach to point estimation for the parameters θ is to recursively maximize the series of likelihoods $p(z_{1:k} | \theta)$. An on-line EM algorithm could be employed for this task, but this requires estimation of sufficient statistics based on probability distributions with increasing dimension with respect to time. Andrieu et al. [7] propose an on-line EM algorithm that focuses on a pseudo-likelihood. The on-line EM updates are performed every L time-steps using blocks of particles and measurements. Define $\mathbf{X}_b \triangleq \mathbf{x}_{bL+1:(b+1)L}$ and $\mathbf{Z}_b \triangleq \mathbf{z}_{bL+1:(b+1)L}$, where b is the index of the block.

Since the underlying process \mathbf{x}_k is stationary, the vectors $\{\mathbf{X}_b, \mathbf{Z}_b\}$ are identically distributed with common distribution

$$p_\theta(\mathbf{X}_b, \mathbf{Z}_b) = \pi_\theta(\mathbf{x}_{bL+1}) p_\theta(\mathbf{z}_{bL+1} | \mathbf{x}_{bL+1}) \times \prod_{k=bL+2}^{(b+1)L} p_\theta(\mathbf{x}_k | \mathbf{x}_{k-1}) p_\theta(\mathbf{z}_k | \mathbf{x}_k) \quad (6)$$

where $\pi_\theta(\cdot)$ is the stationary distribution of the process \mathbf{x} . The likelihood $p_\theta(\mathbf{Z}_b)$ for block b is

$$p_\theta(\mathbf{Z}_b) = \int_{\mathbf{x}^L} p_\theta(\mathbf{x}, \mathbf{Z}_b) d\mathbf{x}. \quad (7)$$

We form an estimate of θ by maximizing a log pseudo-likelihood function [7] defined for m blocks of observations as

$$l(\theta) = \sum_{b=1}^{m-1} \log p_\theta(\mathbf{Z}_b) \quad (8)$$

Under ergodicity assumptions, the average log pseudo-likelihood satisfies

$$\bar{l}(\theta) = \int_{\mathbf{z}^L} \log p_\theta(\mathbf{z}) p_{\theta^*}(\mathbf{z}) d\mathbf{z} \quad (9)$$

where θ^* is the true value of θ . The on-line EM algorithm recursively maximizes $\bar{l}(\theta)$ by updating the estimate of θ via

$$\theta_b = \arg \max_{\theta \in \Theta} Q(\theta, \theta_{b-1}) \quad (10)$$

where

$$Q(\theta, \theta_{b-1}) = \int_{\mathbf{x}^L \times \mathbf{z}^L} \log(p_\theta(\mathbf{x}, \mathbf{z})) p_{\theta_{b-1}}(\mathbf{x} | \mathbf{z}) p_{\theta^*}(\mathbf{z}) d\mathbf{x} d\mathbf{z} \quad (11)$$

In practice, we compute Q via a set of sufficient statistics $\Omega(\theta_b, \theta^*)$. We use $\theta_b = \Lambda(\Omega(\theta_{b-1}, \theta^*))$ as a mapping function

from the sufficient statistics $\Omega(\theta, \theta^*)$ to θ that maximizes Q . In our case, the sufficient statistics $\Omega(\theta_{b-1}, \theta^*)$ are:

$$\begin{aligned}\Omega(\theta_{b-1}, \theta^*) &= [\omega_1, \omega_2, \omega_3, \omega_4] \\ &= E_{\theta_{b-1}, \theta^*}[\psi_1, \psi_2, \psi_3, \psi_4]\end{aligned}\quad (12)$$

where w_1, \dots, w_4 are functions of θ_{b-1} and θ^* , and ψ_1, \dots, ψ_4 are functions of \mathbf{X}_b and \mathbf{Z}_b . The expectation is with respect to $p_{\theta_{b-1}}(\mathbf{x}|\mathbf{z})p_{\theta^*}(\mathbf{z})$.

$$\psi_1(\mathbf{X}_b, \mathbf{Z}_b) = \sum_{k=bL+2}^{(b+1)L} ((\mathbf{x}_k - \mathbf{x}_{k-1})^T (\mathbf{x}_k - \mathbf{x}_{k-1}))$$

$$\psi_2(\mathbf{X}_b, \mathbf{Z}_b) = \sum_{k=bL+1}^{(b+1)L} ((\mathbf{z}_k - \phi \mathbf{g}_k)^T (\mathbf{z}_k - \phi \mathbf{g}_k))$$

$$\psi_3(\mathbf{X}_b, \mathbf{Z}_b) = \sum_{k=bL+1}^{(b+1)L} (\mathbf{z}_k^T \mathbf{g}_k)$$

$$\psi_4(\mathbf{X}_b, \mathbf{Z}_b) = \sum_{k=bL+1}^{(b+1)L} \|\mathbf{g}_k\|_2^2$$

The mapping Λ is defined as:

$$\sigma_{vb} = \sqrt{\frac{\omega_1(\theta_{b-1}, \theta^*)}{2(L-1)}} \quad (13)$$

$$\sigma_{sb} = \sqrt{\frac{\omega_2(\theta_{b-1}, \theta^*)}{ML}} \quad (14)$$

$$\phi_b = \frac{\omega_3(\theta_{b-1}, \theta^*)}{\omega_4(\theta_{b-1}, \theta^*)} \quad (15)$$

The expectations do not have an analytical solution, so we calculate them by an importance sampling approach, using the particle tracks that we generate in our tracking algorithm. The complete algorithm, combining the SIR filter and on-line EM, is described in Algorithm 1 below. For the simulations reported in this paper, we have used the prior $p(\mathbf{x}_k|\mathbf{x}_{k-1}^{(i)})$ as the importance function q .

5. SIMULATION RESULTS

5.1. Simulation Description

In this section we present the results of simulations conducted to explore the performance of the proposed algorithm. The simulation mimics a wireless sensor network with 24 nodes that we have used for preliminary experiments. The sensor nodes are deployed in a $7m \times 7m$ square as shown in Figure 2 (a), with a spacing of 1 metre. A person walks within the network area clockwise along a specified square route (the blue line) with the speed of 0.5 metres per second starting from position (1,1). A set of measurements is recorded every second (i.e. each time step corresponds to one second).

We generate 100 realizations of this trajectory for each of 3 measurement noise standard deviations $\sigma_s = 0.1, 0.5, \sqrt{5}$. The measurements are generated according to two models: the pixel-free model described in this paper and the pixelized model from [2]. For the pixel-free model, $\sigma_\lambda = 0.02$ and $\phi = 5$ (these values were chosen because they provide a good fit to our experimental data). For the pixelized model, $\Delta p = 0.15m$ (pixel width), and $\lambda = 0.02$ (see [2]), and $\phi = 15$ (again these values provide a good fit to experimental data).

We compare the performance of the SMC algorithm with that of the imaging plus Kalman filter algorithm of [3]. In the SMC algorithm, we use 1000 particles. The unknown parameter values in the on-line EM algorithm are initialized by drawing from the following uniform distributions: $\sigma_s \sim U(0, \sqrt{5})$, $\phi \sim U(0, 10)$ and $\sigma_v \sim U(0, 1]$. In the imaging plus Kalman filter algorithm, the regularization parameter α used in the imaging algorithm is set to 200. The transition noise σ_v for the Kalman filter is set to 0.3.

```
// Initialization
Sample  $\theta_0 \sim q(\theta)$  and set  $b = 1$ ;
for  $i = 1, \dots, N$  do
    Sample  $\mathbf{x}_0^{(i)} \sim q(\mathbf{x}_0)$ ;
    Set  $w_0^{(i)} = \frac{p(\mathbf{x}_0^{(i)})}{q(\mathbf{x}_0^{(i)})}$ ;
end
for  $k = 1, 2, \dots$  do
    // SIR
    for  $i = 1, \dots, N$  do
        // Sampling
        Sample  $\mathbf{x}_k^{(i)} \sim q_{\theta_{b-1}}(\mathbf{x}_k|\mathbf{x}_{k-1}^{(i)}, \mathbf{z}_k)$ ;
        // Calculate importance weights
        Set  $\rho_k^{(i)} = \frac{p_{\theta_{b-1}}(\mathbf{z}_k|\mathbf{x}_k^{(i)})p_{\theta_{b-1}}(\mathbf{x}_k|\mathbf{x}_{k-1}^{(i)})}{q_{\theta_{b-1}}(\mathbf{x}_k|\mathbf{x}_{k-1}^{(i)}, \mathbf{z}_k)}$ ;
    end
    // Resample
    Resample  $\{\mathbf{x}_k^{(i)}, \rho_k^{(i)}\}_{i=1}^N$  to obtain  $\{\mathbf{x}_k^{(i)}, \frac{1}{N}\}_{i=1}^N$ 

    // On-line EM
    if  $k \bmod L = 0$  then
        // E-step
        for  $i = 1, \dots, N$  do
            Calculate  $W_b^{(i)} = \frac{p_{\theta_{b-1}}(\mathbf{x}_b^{(i)}|\mathbf{z}_b)}{q_{\theta_{b-1}}(\mathbf{x}_b^{(i)}|\mathbf{z}_b)}$ ;
        end
        Normalize weights  $\{W_b^{(i)}\}$  such that
         $\sum_{i=1}^N W_b^{(i)} = 1$ ;
        Update  $\hat{\Omega}_b =$ 
         $(1 - \alpha_b)\hat{\Omega}_{b-1} + \alpha_b \sum_{m=1}^N W_b^{(m)}\psi(\mathbf{X}_b^{(m)}, \mathbf{Z}_b)$ ;
        // M-step
        Set  $\theta_b = \Lambda(\hat{\Omega}_b)$  and  $b = b + 1$ ;
    end
end
```

Algorithm 1: SMC RF Tomographic Tracking

5.2. Results

An example SMC-estimated trajectory for the case $\sigma_s = \sqrt{5}$ is shown in Figure 2; it clearly provides a relatively accurate approximation of the ground-truth trajectory. Figure 3 shows a box-and-whisker plot of the mean-squared error (MSE) for the SMC algorithm when applied to data generated using the pixel-free model, based on 100 realizations. The MSE decreases rapidly after the first 10 time steps and stays at a constant low level. For almost all tracks, the on-line EM succeeds in providing acceptably accurate estimates of the unknown parameters, leading to improved performance over

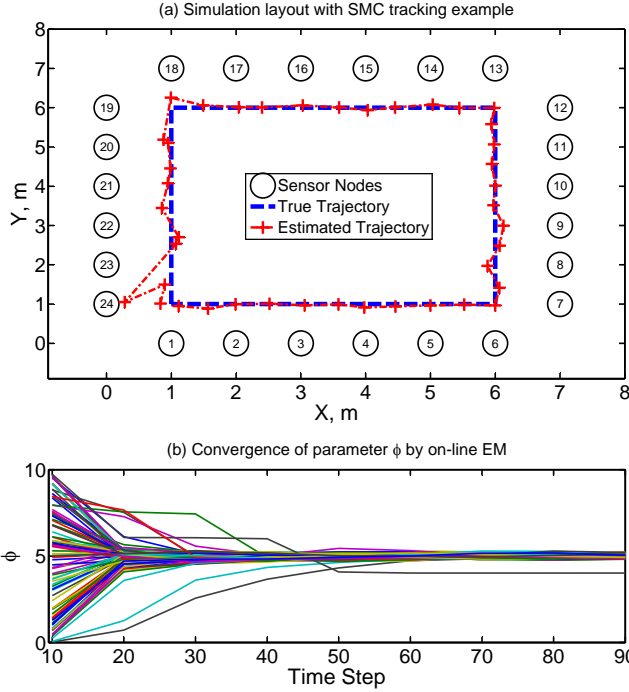


Fig. 2. Simulation scenario with a square trajectory. (a) An example tracking estimate is depicted for the case $\sigma_s = \sqrt{5}$. (b) The evolution of the estimate of ϕ using the on-line EM algorithm. For most tracks the estimates converge to a value close to the true value of 5.

time. Figure 2(b) shows the evolution of the estimates of ϕ . Almost all estimates converge to values close to the true value 5 after 30-40 seconds (3-4 update steps in on-line EM).

Tables 1 and 2 compare the mean-squared error (MSE) of the SMC and the imaging plus KF algorithms using the data generated from the pixelized model and the pixel-free model, respectively. At the same noise level, the MSE values of SMC algorithm are much lower than those of the imaging plus KF algorithm. The SMC algorithm, despite operating under the assumption of a pixel-free model, significantly outperforms the imaging plus KF algorithm even when the data is generated using a pixelized model.

Noise Std. Dev.	SMC Alg. (m^2)	Imaging Alg. (m^2)
0.5	0.0086	0.6165
1	0.0093	0.6166
$\sqrt{5}$	0.0158	0.6645

Table 1. MSE comparison using data from pixelized model

Noise Std. Dev.	SMC Alg. (m^2)	Imaging Alg. (m^2)
0.5	0.0010	0.0943
1	0.0019	0.4890
$\sqrt{5}$	0.0277	2.2046

Table 2. MSE comparison using data from pixel-free model

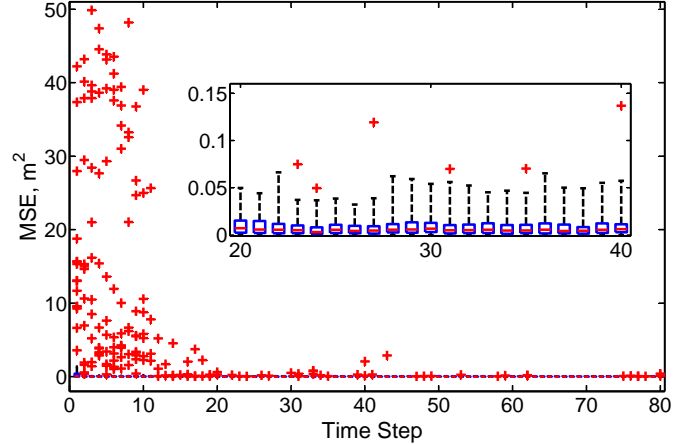


Fig. 3. Box-and-whisker plot of the MSE as a function of time for the SMC algorithm applied to data generated using the pixel-free model. The boxes range from the 25th to 75th quantiles; the whiskers extend 3 times the interquartile range. The median is marked as a red line; and the red plus symbols indicate outliers.

6. CONCLUSIONS

This paper introduces a particle filtering method for RF tomographic tracking of a single target. The algorithm incorporates an on-line EM algorithm to estimate key parameters in the measurement and dynamic models. In order to improve the accuracy and to reduce computational requirements, we developed a pixel-free measurement model based on experimental data. Simulation results demonstrate that the algorithm is effective and outperforms the previously described approach. Future work will focus on real-world experiments and an extension to multi-target tracking.

7. REFERENCES

- [1] M. Moussa and M. Youssef, "Smart devices for smart environments: Device-free passive detection in real environments," in *Proc. Int. Conf. Perv. Comp. and Comm.*, Galveston, TX, U.S.A., Mar. 2009.
- [2] J. Wilson and N. Patwari, "Radio tomographic imaging with wireless networks," *IEEE Trans. Mobile Computing*, vol. 9, no. 5, pp. 621–632, Jan. 2010.
- [3] J. Wilson and N. Patwari, "See Through Walls: Motion Tracking Using Variance-Based Radio Tomography Networks," to appear, *IEEE Trans. Mobile Computing*, 2010.
- [4] M. Kanso and M. Rabbat, "Compressed RF Tomography for Wireless Sensor Networks: Centralized and Decentralized Approaches," in *Proc. IEEE Dist. Computing in Sensor Systems*, Santa Barbara, U.S.A., June 2010.
- [5] D. Zhang, J. Ma, Q. Chen, and L.M. Ni, "An RF-based system for tracking transceiver-free objects," in *Proc. IEEE Int. Conf. Perv. Comp. and Comm.*, White Plains, NY, U.S.A., Mar. 2007.
- [6] A. Doucet and M. Johansen, *Oxford Handbook of Nonlinear Filtering*, chapter A tutorial on particle filtering and smoothing: fifteen years later, Oxford University Press, 2010, to appear.
- [7] C. Andrieu, A. Doucet, and V.B. Tadic, "On-line parameter estimation in general state-space models," in *Proc. IEEE Conf. on Decision and Control*, Seville, Spain, Jan. 2006.